Chapter 4: Turbulence at Small Scales
Part 8: Structure functions

6.1.4 *Restatement of the Kolmogorov hypotheses*

In order to deduce precise consequences from them, it is worthwhile to provide here more precise statements of the Kolmogorov (1941) hypotheses. Kolmogorov presented these in terms of an N-point distribution in the four-dimensional x–t space. Here, however, we consider the N-point distribution in physical space ($\boldsymbol{x}$) at a fixed time t – which is sufficiently general for most purposes.

Consider a simple domain $\mathcal{G}$ within the turbulent flow, and let $\boldsymbol{x}^{(0)}$, $\boldsymbol{x}^{(1)}, \ldots, \boldsymbol{x}^{(N)}$ be a specified set of points within $\mathcal{G}$. New coordinates and velocity differences are defined by

$$\boldsymbol{y} \equiv \boldsymbol{x} - \boldsymbol{x}^{(0)}, \tag{6.20}$$

$$\boldsymbol{v}(\boldsymbol{y}) \equiv \boldsymbol{U}(\boldsymbol{x}, t) - \boldsymbol{U}(\boldsymbol{x}^{(0)}, t), \tag{6.21}$$

and the joint PDF of $\boldsymbol{v}$ at the N points $\boldsymbol{y}^{(1)}, \boldsymbol{y}^{(2)}, \ldots, \boldsymbol{y}^{(N)}$ is denoted by f_N.

The definition of local homogeneity. The turbulence is locally homogeneous in the domain $\mathcal{G}$, if for every fixed N and $\boldsymbol{y}^{(n)} (n = 1, 2, \ldots, N)$, the N-point PDF f_N is independent of $\boldsymbol{x}^{(0)}$ and $\boldsymbol{U}(\boldsymbol{x}^{(0)}, t)$.

The definition of local isotropy. The turbulence is locally isotropic in the domain $\mathcal{G}$ if it is locally homogeneous and if in addition the PDF f_N is invariant with respect to rotations and reflections of the coordinate axes.

The hypothesis of local isotropy. In any turbulent flow with a sufficiently large Reynolds number ($\mathrm{Re} = \mathcal{UL}/\nu$), the turbulence is, to a good approximation, locally isotropic if the domain $\mathcal{G}$ is sufficiently small (i.e., $|\boldsymbol{y}^{(n)}| \ll \mathcal{L}$, for all n) and is not near the boundary of the flow or its other singularities.

The first similarity hypothesis. For locally isotropic turbulence, the N-point PDF f_N is uniquely determined by the viscosity ν and the dissipation rate ε.

The second similarity hypothesis. If the moduli of the vectors $\boldsymbol{y}^{(m)}$ and of their differences $\boldsymbol{y}^{(m)} - \boldsymbol{y}^{(n)}$ ($m \neq n$) are large compared with the Kolmogorov scale η, then the N-point PDF f_N is uniquely determined by ε and does not depend on ν.

It is important to observe that the hypotheses apply specifically to velocity differences. The use of the N-point PDF f_N allows the hypotheses to be applied to any turbulent flow, whereas statements in terms of wavenumber spectra apply only to flows that are statistically homogeneous (in at least one direction).

For inhomogeneous flows, local isotropy is possible only 'to a good approximation' (as stated in the hypothesis). For example, taking $\boldsymbol{y}^{(1)} = \boldsymbol{e}\ell$ and $\boldsymbol{y}^{(2)} = -\boldsymbol{e}\ell$ (where ℓ is a specified length and $\boldsymbol{e}$ a specified unit vector), we have

$$\begin{aligned} \langle \boldsymbol{v}(\boldsymbol{y}^{(1)}) - \boldsymbol{v}(\boldsymbol{y}^{(2)}) \rangle &= \langle \boldsymbol{U}(\boldsymbol{y}^{(1)}) \rangle - \langle \boldsymbol{U}(\boldsymbol{y}^{(2)}) \rangle \\ &\approx 2 \frac{\ell}{\mathcal{L}} \boldsymbol{e} \cdot \mathcal{L} \nabla \langle \boldsymbol{U} \rangle. \end{aligned} \tag{6.22}$$

Evidently this simple statistic is not exactly isotropic, but instead has a small anisotropic component – of order $\ell/\mathcal{L}$ – arising from large-scale inhomogeneities.

6.2 Structure functions

To illustrate the correct application of the Kolmogorov hypotheses, we consider – as did Kolmogorov (1941b) – the second-order velocity structure functions. The predictions of the hypotheses are deduced, and then compared with experimental data.

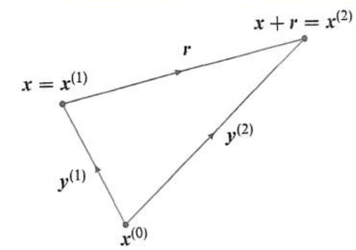

Fig. 6.3. A sketch showing the points x and $x + r$ in terms of $x^{(n)}$ and $y^{(n)}$. All points are within the domain $\mathcal{G}$.

By definition, the second-order velocity structure function is the covariance of the difference in velocity between two points $x + r$ and x:

$$D_{ij}(r, x, t) \equiv \langle [U_i(x + r, t) - U_i(x, t)][U_j(x + r, t) - U_j(x, t)] \rangle. \qquad (6.23)$$

6.3 Two-point correlation

The Kolmogorov hypotheses, and deductions drawn from them, have no direct connection to the Navier–Stokes equations (although, as in the previous section, the continuity equation is usually invoked). Although, in the description of the energy cascade, the transfer of energy to successively smaller scales has been identified as a phenomenon of prime importance, the precise mechanism by which this transfer takes place has not been identified or quantified. It is natural, therefore, to try to extract from the Navier–Stokes equations useful information about the energy cascade. The earliest attempts

(outlined in this section) are those of Taylor (1935a) and of von Kármán and Howarth (1938), which are based on the two-point correlation. The next two sections give the view from wavenumber space in terms of the energy spectrum – the Fourier transform of the two-point correlation.

Autocorrelation functions

Consider homogeneous isotropic turbulence, with zero mean velocity, r.m.s. velocity $u'(t)$, and dissipation rate $\varepsilon(t)$. Because of homogeneity, the two-point correlation

$$R_{ij}(r, t) \equiv \langle u_i(x + r, t) u_j(x, t) \rangle, \qquad (6.41)$$

is independent of x. At the origin it is

$$R_{ij}(0, t) = \langle u_i u_j \rangle = u'^2 \delta_{ij}. \qquad (6.42)$$

Kolmogorov spectra can be obtained via two paths:

1. Use Fourier transforms of structure functions (physical space)
2. Apply Kolmogorov hypothesis directly to the spectra (wave number space)

The second approach is less rigorous but simpler as we have done. The first approach was originally used by Kolmogorov.

Second order velocity structure function is co-variance of the difference in velocity between two points $\underline{x} + \underline{r}$ and x: 2nd order tensor which is determined by all eddies with size less than or comparable with $\underline{r}$.

$$D_{ij}(\underline{x}, \underline{r}, \tau) = \overline{[u_i(\underline{x} + \underline{r}, t) - u_i(\underline{x}, t)][u_j(\underline{x} + \underline{r}, t) - u_j(\underline{x}, t)]}$$

To within scalar multiples, the only second-order tensors that can be formed from the vector $\underline{r}$ are δ_{ij} and $r_i r_j$. Consequently D_{ij} can be written as

$$D_{ij}(\underline{r}, t) = D_{NN}(r, t)\delta_{ij} + [D_{LL}(r, t) - D_{NN}(r, t)]\frac{r_i r_j}{r^2}$$

Where the scalar functions D_{LL} and D_{NN} are called, respectively, the longitudinal and transverse structure functions. If the coordinate system is chosen so that $\underline{r} = r\widehat{e_1}$

$$D_{11} = D_{LL} \quad D_{22} = D_{33} = D_{NN} \quad D_{ij} = 0 \;\; i \neq j$$

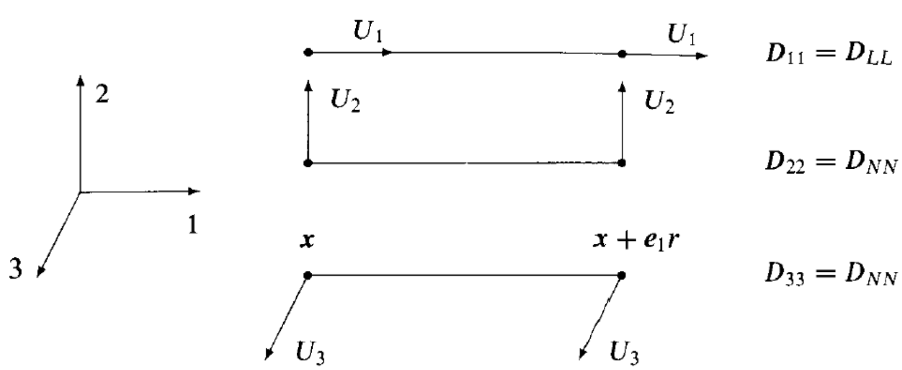

Fig. 6.4. A sketch of the velocity components involved in the longitudinal and transverse structure functions for $\boldsymbol{r} = \boldsymbol{e}_1 r$.

As for $\mathcal{R}_{ij}$,

$$\frac{\partial}{\partial r_j} D_{ij} = 0 \quad \text{Due to incompressibility}$$

Combining isotropic theory with the incompressibility condition

$$D_{NN}(r,t) = D_{LL}(r,t) + \frac{1}{2} r \frac{\partial}{\partial r} D_{LL}(r,t)$$

i.e., $D_{ij}(\underline{r},t) = f\left(D_{LL}(r,t)\right)$ determined by simple scalar function.

According to the 1st similarity hypothesis, given $\underline{r}\ \left(|\underline{r}| \ll L\right)$, D_{ij} is uniquely determined by ε and ν.

$(\varepsilon r)^{2/3}$ has dimensions of velocity squared, and so can be used to make D_{ij} non-dimensional. There is only one independent non-dimensional group that can be formed from r, ε, ν which can be taken to be $r\varepsilon^{1/4}\nu^{3/4} = r/\eta$, where $\eta = \varepsilon^{-1/4}\nu^{-3/4}$.

Thus,

$$D_{LL}(r,t) = (\varepsilon r)^{2/3} \widehat{D}_{LL}(r/\eta)$$

where $\widehat{D}_{LL}(r/\eta)$ is a universal, non-dimensional function.

According to the 2nd similarity hypothesis, for large r/η $(L \gg r \gg \eta)$, D_{LL} is independent of ν and there is no non-dimensional group that can be formed from ε and r

$$D_{LL}(r,t) = C_2(\varepsilon r)^{2/3}$$

Where C_2 is a universal constant → For large r/η, $\widehat{D}_{LL}(r/\eta)$ asymptotically goes to a constant value C_2.

$$D_{NN}(r,t) = \frac{4}{3}D_{LL}(r,t) = \frac{4}{3}C_2(\varepsilon r)^{2/3} \qquad \text{in inertial subrange}$$

$$D_{ij}(\underline{r},t) = C_2(\varepsilon r)^{2/3}\left(\frac{4}{3}\delta_{ij} - \frac{1}{3}\frac{r_i r_j}{r^2}\right) = f(C_2, \varepsilon, r)$$

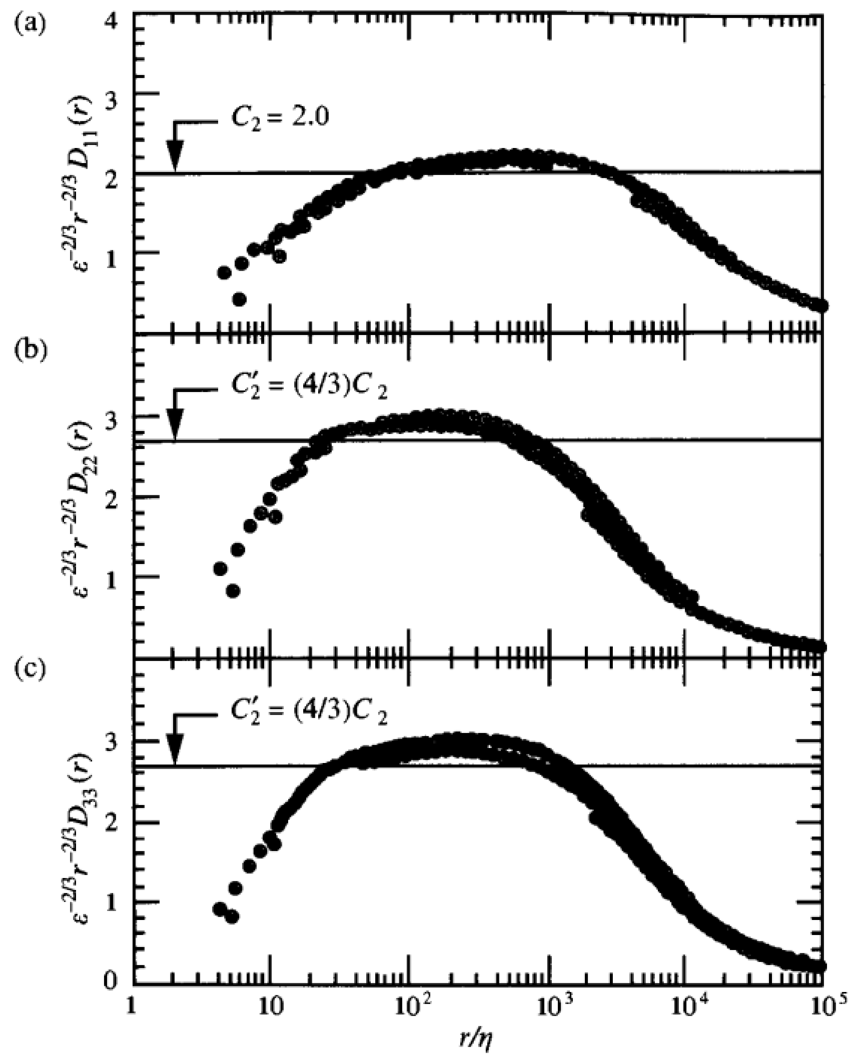

Fig. 6.5. Second-order velocity structure functions measured in a high-Reynolds-number turbulent boundary layer. The horizontal lines show the predictions of the Kolmogorov hypotheses in the inertial subrange, Eqs. (6.33) and (6.34). (From Sad-doughi and Veeravalli (1994).)

the above predictions can readily be examined. Taking the value $C_2 = 2.0$ suggested by these and other data, we draw the following conclusions.

(i) For 7,000 $\eta \approx \frac{1}{2}\mathcal{L} > r > 20\eta$, $D_{11}/(\varepsilon r)^{2/3}$ is within $\pm 15\%$ of C_2.

(ii) There is no perceptible difference between D_{22} and D_{33}.

(iii) For 1,200 $\eta \approx \frac{1}{10}\mathcal{L} > r > 12\eta$, $D_{22}/(\varepsilon r)^{2/3}$ is within $\pm 15\%$ of $\frac{4}{3}C_2$.

Over the ranges of r given above, D_{11} and D_{22} change by factors of 50 and 20, respectively, and so $\pm 15\%$ variations can be considered small in comparison.

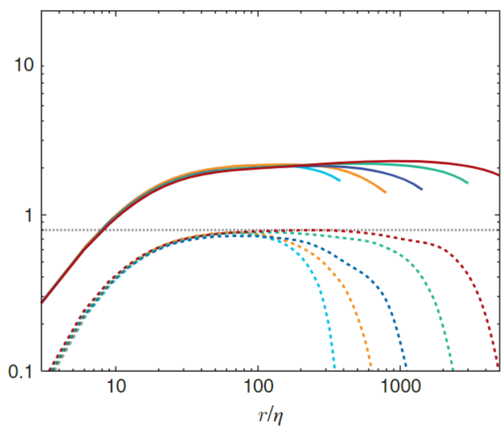

Figure 4.10 Compensated longitudinal structure functions computed in isotropic turbulence [24]. $S_2^L/(\epsilon_r r)^{2/3}$, top curves; $-S_3^L/(\epsilon_r r)$, bottom curves. Constant, dotted line is 0.8. The sequence of curves in each group covers an increasing r/η domain correspond to $R_\lambda = 167, 257, 471, 732, 1131$.

Figure shows the compensated structure functions $S_2^L(r)/(\overline{\varepsilon_r}r)^{2/3}$and $-S_3^L(r)/(\overline{\varepsilon_r}r)$ with $\eta = (\nu^3/\varepsilon)^{1/4}$

Compensated structure functions nearly constant for $\frac{r}{\eta} > \frac{100}{\eta}$ which is appropriate for inertial subrange.

The constant values achieved by the curves match the coefficients in Bernard Eq. (4.101) and (4.102), but there is a slight tilt, such that the observed power laws are close to an $r^{n/3}$ behavior, but do not exactly have this trend.

This suggests that $\alpha(2/3)$ and $\alpha(1)$ do not vanish. Measurements of structure functions for larger n show that the departure from $r^{n/3}$ behavior becomes more significant.

The trends in $S_n^L(r)$ are the physical space analogue to the discrepancies in the -5/3 wave number spectrum in Figure 4.8. Also in this case, it is believed that these are a consequence of intermittency.

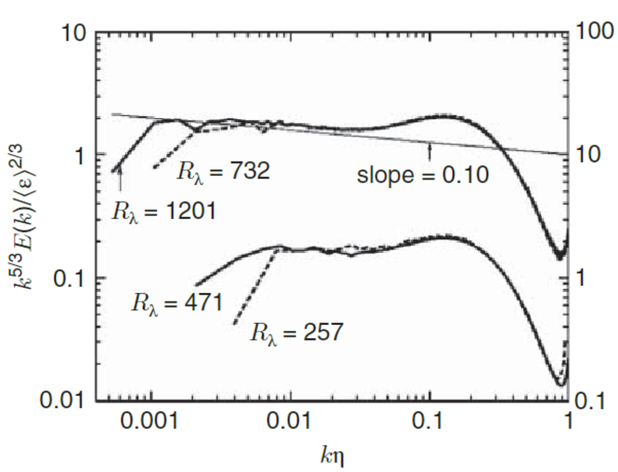

Figure 4.8 Compensated energy spectrum as given in [21]. With increasing R_λ the simulations used 512^3, 1024^3, 2048^3, and 4096^3 meshes. Scales on the left and right are for the upper and lower curves, respectively. Reproduced from *Physics of Fluids*, Vol. 15, pp. L21–L24, 2003, with the permission of AIP Publishing.